Journal of Chromatography A 1731 (2024) 465156

Contents lists available at ScienceDirect

Journal of Chromatography A

journal homepage: www.elsevier.com/locate/chroma

Short communication

Enhancing thermodynamic consistency: Clarification on the application of asymmetric activity model in multi-component chromatographic separation

Yu-Cheng Chen, Shan-Jing Yao, Dong-Qiang Lin *

Key Laboratory of Biomass Chemical Engineering of Ministry of Education, Zhejiang Key Laboratory of Smart Biomaterials, College of Chemical and Biological Engineering, Zhejiang University, Hangzhou 310058, China

ARTICLE INFO

Keywords:
Thermodynamic model
Mechanistic model
Chromatography
Activity coefficient

ABSTRACT

The single-component Mollerup model, with over 40 direct applications and 442 citations, is the most widely used activity model for chromatographic mechanistic modeling. Many researchers have extended this formula to multi-component systems by directly adding subscripts, a modification deemed thermodynamically inconsistent (referred to as the reference model). In this work, we rederived the asymmetric activity model for multi-component systems, using the van der Waals equation of state, and termed it the multi-component Mollerup model. In contrast to the reference model, our proposed model accounts for the contributions of all components to the activity. Three numerical experiments were performed to investigate the impact of the three different activity models on the chromatographic modeling. The results indicate that our proposed model represents a thermodynamically consistent generalization of the single-component Mollerup model to multi-component systems. This communication advocates adopting of the multi-component Mollerup model for activity modeling in multi-component chromatographic separation to enhance thermodynamic consistency.

1. Introduction

Hydrophobic interactions and ionic interactions are two typical forces between the adsorbate components and the chromatographic adsorbent. These interactions give rise to hydrophobic interaction chromatography (HIC) and ion-exchange chromatography (IEC), respectively, while their coupling leads to mixed-mode chromatography (MMC). Reversed-phase chromatography (RPC) is another mode yielded from hydrophobic interactions. Modeling the chromatographic process based on these interaction mechanisms has garnered significant research interest.

Let c_i and q_i represent the adsorbate concentrations in the mobile phase and stationary phase, respectively, while c_m and q_m represent the modifier concentrations in the mobile phase and stationary phase, respectively. $k_{\mathrm{kin},i}$, $k_{\mathrm{eq},i}$, and ν_i represent the kinetic coefficient, equilibrium coefficient, and characteristic charge, respectively. The adsorption isotherm models corresponding to hydrophobic interactions and ionic interactions can be expressed as follows:

$$k_{\mathrm{kin},i}\cdot\frac{\partial q_i}{\partial t} = k_{\mathrm{eq},i}\cdot\overline{q}_\mathrm{m}^{\nu_i}\cdot c_i - q_i \tag{1}$$

$$k_{\mathrm{kin},i}\cdot\frac{\partial q_i}{\partial t} = k_{\mathrm{eq},i}\cdot\overline{q}_\mathrm{m}^{\nu_i}\cdot c_i - q_i\cdot c_\mathrm{m}^{\nu_i} \tag{2}$$

The type of modifier depends on the chromatographic modes. For HIC and IEC, the modifier can be a salt solution such as NaCl. For RPC, the modifier can be a solvent such as acetonitrile.

By modifying $k_{\mathrm{eq},i}$ and the nonlinear terms $\overline{q}_\mathrm{m}^{\nu_i}$ in Eqs. (1) and (2), most well-established chromatographic models can be derived as shown in Table 1. Among these models, those that consider activity corrections, such as the Mollerup-HIC, generalized ion-exchange (GIEX), and self-association (SAS) models, are more broadly applicable due to their consideration of solution non-ideality.

The simulation results of the models depend on the choice of the activity model. Currently, the activity model with coefficients $\widetilde{\gamma}_i$ proposed by Mollerup [1] is widely used. Table 2 lists forty research papers that have adopted the Mollerup model up to June 2024. This activity model is based on the van der Waals equation of state given by Eq. (3-70)

---

* Corresponding author.
E-mail address: lindq@zju.edu.cn (D.-Q. Lin).

https://doi.org/10.1016/j.chroma.2024.465156
Received 28 May 2024; Received in revised form 6 July 2024; Accepted 8 July 2024

in Prausnitz, et al. [2]. For a mixture system containing one component (protein), one solvent (water), and one modifier (salt), the activity model is expressed as:

$$\ln\widetilde{\gamma} = k_s c_s + k_p c_p \tag{3}$$

which is referred to as the single-component Mollerup model in this work. k_s and k_p are interaction parameters of salts and proteins, respectively. Since the initial proposal of Eq. (3) in 2006, it has had a significant impact on the chromatographic mechanistic modeling, with over 40 direct applications and 442 citations (all citations are listed in the Supporting Information and include only research articles).

When extending Eq. (3) to multi-component systems, many researchers have adopted a straightforward subscript modification:

$$\ln\widetilde{\gamma}_i = k_{s,i} c_s + k_{p,i} c_{p,i} \tag{4}$$

which is referred to as the reference model. We argue that this modification is not coherent with the van der Waals equation of state used to derive the model. A more reasonable and thermodynamically consistent expression should be:

$$\ln\widetilde{\gamma}_i = k_{s,i} c_s + \sum_{j=1}^{n} k_{p,ij} c_{p,j} \tag{5}$$

Extending Eq. (5) to more general systems beyond salts and proteins, i.e., a mixture system containing n components (solutes except for the modifier), one solvent (water), and one modifier, the expression is written as:

$$\ln\widetilde{\gamma}_i = k_{m,i} c_m + \sum_{j=1}^{n} k_{ij} c_j \tag{6}$$

which is named as the multi-component Mollerup model.

In this study, we will rederive the asymmetric activity model for multi-component systems using the van der Waals equation of state and elucidate the underlying mechanisms behind our derivations. Through numerical experiments, our proposed multi-component Mollerup model will be compared with the reference model for multi-component chromatographic modeling. Furthermore, we will confirm that our proposed model represents a thermodynamically consistent generalization of the single-component Mollerup model to multi-component systems. Finally, the impact of different loadings on these models will be evaluated.

2. Theory

Let us return to the van der Waals equation of state for incompressible fluids, which was used to derive the single-component Mollerup model in Eq. (3):

$$\ln\widehat{\varphi}_i = \ln\frac{\upsilon}{\upsilon - b} + \frac{b_i}{\upsilon - b} - \frac{2\sqrt{a_i}\left(y_w\sqrt{a_w} + y_m\sqrt{a_m} + \sum_{j=1}^{n} y_j\sqrt{a_j}\right)}{\upsilon RT} \tag{7}$$

where $\widehat{\varphi}_i$ is the fugacity coefficient, υ is the molar volume, R is the gas constant, T is the temperature in kelvin, y_j is the mole fraction, and a and b are the constants dependent on composition.

The definition of the asymmetric activity coefficient is given by

$$\widetilde{\gamma}_i = \frac{\gamma_i}{\lim\limits_{y_i \to 0}\gamma_i} = \frac{\widehat{\varphi}_i}{\lim\limits_{y_i \to 0}\widehat{\varphi}_i} \tag{8}$$

where $\lim\limits_{y_i \to 0}\widehat{\varphi}_i$ represents the fugacity coefficient at infinite dilution in pure water (without the modifier). Denoting $\sqrt{a_i}\sqrt{a_j}$ as a_{ij} and combining Eqs. (7) and (8), one can obtain

$$\ln\widetilde{\gamma}_i = \frac{2}{\upsilon RT}\left(a_{iw} - y_w a_{iw} - y_m a_{im} - \sum_{j=1}^{n} y_j a_{ij}\right) \tag{9}$$

Based on Mollerup [1]'s assumption that the solute mole fractions are small, $y_w \approx 1$. For the liquid phase, let x_j represent the mole fraction. Thus, Eq. (9) can be simplified to:

$$\ln\widetilde{\gamma}_i = -\frac{2}{\upsilon RT}\left(x_m a_{im} + \sum_{j=1}^{n} x_j a_{ij}\right) \tag{10}$$

where if $k_{ij} = -\frac{2a_{ij}}{\upsilon RTc_w}$ and c_w represents the molar concentration of water at standard ambient temperature and pressure, approximately 55.6 mol/L, Eq. (10) can be rewritten as Eq. (6).

When there is only one component present in the solution, Eq. (6) is equivalent to the single-component Mollerup model in Eq. (3). In the

Table 1

Well-established chromatographic models by modify $k_{eq,i}$ and $\overline{q}_m^{\nu_i}$.

Model	Base equation	Modified $k_{eq,i}$	Modified $\overline{q}_m^{\nu_i}$	Introduced parameters
Linear	Eq. (1)	$k_{eq,i}$	1	–
Langmuir	Eq. (1)	$k_{eq,i}$	$q_{max,i}\left(1 - \sum_{j=1}^{n}\frac{q_j}{q_{max,j}}\right)$	q_{max}
Salt-dependent Langmuir	Eq. (2)	$k_{eq,i}$	$q_{max,i}\left(1 - \sum_{j=1}^{n}\frac{q_j}{q_{max,j}}\right)$	q_{max}
Stoichiometric displacement model (SDM)	Eq. (2)	$k_{eq,i}$	$\Lambda^{\nu_i}\left(1 - \sum_{j=1}^{n}\frac{q_j}{\Lambda/\nu_j}\right)^{\nu_i}$	Λ capacity $k_{D,i}$ equilibrium coefficient for dimerization
Steric mass action (SMA)	Eq. (2)	$k_{eq,i}$	$\Lambda^{\nu_i}\left[1 - \sum_{j=1}^{n}\frac{q_j}{\Lambda/(\nu_j + \sigma_j)}\right]^{\nu_i}$	Λ capacity σ shielding factor
Mollerup-HIC[*]	Eq. (1)	$\widetilde{\gamma}_i k_{eq,i}$	$\Lambda^{\nu_i}\left[1 - \sum_{j=1}^{n}\frac{q_j}{\Lambda/(\nu_j + \sigma_j)}\right]^{\nu_i}$	Λ capacity σ shielding factor $\widetilde{\gamma}_i$ assymmetric activity coefficient
Generalized ion-exchange (GIEX)[*]	Eq. (2)	$\widetilde{\gamma}_i k_{eq,i}$	$\Lambda^{\nu_i}\left[1 - \sum_{j=1}^{n}\frac{q_j}{\Lambda/(\nu_j + \sigma_j)}\right]^{\nu_i}$	Λ capacity σ shielding factor $\widetilde{\gamma}_i$ assymmetric activity coefficient
Self-association (SAS)	Eq. (2)	$\left(\widetilde{\gamma}_i + 2k_{D,i}c_i\widetilde{\gamma}_i^2/c\right)k_{eq,i}$[†]	$\Lambda^{\nu_i}\left[1 - \sum_{j=1}^{n}\frac{q_j}{\Lambda/(\nu_j + \sigma_j)}\right]^{\nu_i}$	Λ capacity σ shielding factor $\widetilde{\gamma}_i$ assymmetric activity coefficient

[*] Although the Mollerup-HIC and GIEX models suggest they are specific to certain chromatography modes (the words HIC and IEC in their names), they can also be applied to RPC and MMC [10–13].

[†] Some literature expresses $\left(\widetilde{\gamma}_i + 2k_{D,i}c_i\widetilde{\gamma}_i^2/c\right)k_{eq,i}$, where c is the total molar concentration in the solution, $c \approx c_w \approx 55.6$ mol/L.

case of multiple components present in the solution, Eq. (6) accounts for the contribution of interactions among all solutes to the solution activity compared to the reference model in Eq. (4). The number of model parameters for Eq. (6) is calculated using the combination number C:

$$C(n,1) + C(n,2) + C(n,1) = n(n-1)/2 + 2n \tag{11}$$

Table 3 lists several simplified models of Eq. (6) and the corresponding number of model parameters. The number of model parameters for the reference model in Eq. (4) is $2n$.

3. Methods and materials

3.1. Numerical experiments

This study applied three numerical experiments to investigate the impact of three different activity models on chromatographic mechanistic modeling including the GIEX model (Table 1) coupled with the single-component Mollerup model in Eq. (3), the reference model in Eq. (4), and our proposed multi-component Mollerup model (the two-parameter form $\bar{k}_s c_s + \bar{k}_p \sum_{j=1}^{n} c_j$ as listed in Table 3) in Eq. (6). The investigated multi-component systems comprise a salt and three

Table 2
Research papers using the Mollerup asymmetric activity model up to June 2024.

No.	Chromatography	Separation system	Component	Reference
1	HIC	Lysozyme	Single	Mollerup [1]
2	HIC	Lysozyme	Single	Mollerup [14]
3	HIC	β-lactoglobulin	Single	Mollerup [15]
4	IEC	β-lactoglobulin	Single	Mollerup [15]
5	HIC	α-lactalbumin Carbonic anhydrase Cytochrome c Lysozyme Ovalbumin Ribonuclease a	Single	Deitcher, et al. [16]
6	MMC	α-chymotrypsin Amyloglucosidase Bovine serum albumin Lysozyme Ovalbumin	Single	Nfor, et al. [5]
7	MMC	Amyloglucosidase Bovine Serum Albumin Ovalbumin	Single	Nfor, et al. [6]
8	IEC	Industrial protein	Multiple	Westerberg, et al. [17]
9	HIC	Monoclonal antibody	Single	Nfor, et al. [18]
10	IEC/HIC	α-lactalbumin β-lactoglobulin Bovine serum albumin	Multiple	Nfor, et al. [19]
11	IEC/HIC	Monoclonal antibody	Multiple	Nfor, et al. [20]
12	MMC	Peptide	Single	Chilamkurthi, et al. [21]
13	HIC	Numerical study	Single	Holmqvist, et al. [22]
14	HIC	α-lactalbumin Bovine serum albumin Human serum albumin Trypsinogen	Single	Mirani and Rahimpour [23]
15/16	MMC	Monoclonal antibody	Single	Wang, et al. [7], Wilson, et al. [24]
17	HIC	Industrial protein	Multiple	Hanke, et al. [25]
18	HIC	Insulin	Multiple	Holmqvist and Magnusson [26]
19	MMC	Monoclonal antibody	Single	Lee, et al. [27]
20	IEC	Monoclonal antibody	Single	Huuk, et al. [28]
21	IEC/HIC/MMC	Bispecific antibody	Single	Lee, et al. [29]
22	IEC/HIC	Monoclonal antibody	Multiple	Pirrung, et al. [30]
23	IEC/MMC	Monoclonal antibody	Multiple	Pirrung, et al. [31]
24	IEC	Monoclonal antibody	Multiple[*]	Briskot, et al. [32]
25	HIC	Antibody-drug conjugates	Multiple	Andris and Hubbuch [33]
26	MMC	Numerical study	Multiple	Bock, et al. [34]
27	IEC/MMC	Napin Cruciferin	Single	Moreno-González, et al. [8]
28	HIC	Lysozyme	Single	Lietta, et al. [35]
29	IEC	Peptide	Single	Koch, et al. [9]
30	IEC	Bispecific antibody	Single	Seelinger, et al. [36]
31	MMC	mRNA	Multiple	Mouellef, et al. [37]
32	IEC	Peptide	Single	Koch, et al. [38]
33	MMC	Monoclonal antibody	Single	Hess, et al. [39]
34	Protein A	Monoclonal antibody	Single	Hahn, et al. [40]
35	MMC	Monoclonal antibody	Single	Hahn, et al. [41]
36	MMC	Monoclonal antibody	Single	Altern, et al. [42]
37	MMC	Monoclonal antibody	Single	Hess, et al. [43]
38	HIC	Lysozyme	Single	Yang, et al. [44]
39	MMC	Monoclonal antibody	Multiple	Altern, et al. [45]
40	HIC	Lysozyme Cytochrome c	Multiple	Yang, et al. [46]

[*] The activity model used by the author is Eq. (5).

Table 3

Asymmetric activity coefficients in multi-component systems.

$\ln\widetilde{\gamma}_i$	Interaction between different components (excluding modifier) is unity?	Interaction between components and modifier is unity?	Lower adsorbate concentration?	Number of interaction parameters
$k_{\mathrm{m},i}c_{\mathrm{m}} + \sum_{j=1}^{n} k_{ij}c_j$	–	–	–	$n(n+3)/2$
$k_{\mathrm{m},i}c_{\mathrm{m}} + \overline{k}\sum_{j=1}^{n} c_j$	Yes	–	–	$n+1$
$\overline{k}_{\mathrm{m}}c_{\mathrm{m}} + \overline{k}\sum_{j=1}^{n} c_j$	Yes	Yes	–	2
$k_{\mathrm{m},i}c_{\mathrm{m}}$	–	–	Yes	n
$\overline{k}_{\mathrm{m}}c_{\mathrm{m}}$	–	Yes	Yes	1

components, including weakly adsorbed impurity (W), product (P), strongly adsorbed impurity (S), totally four solutes.

The first numerical experiment compared our proposed model with the reference model in overlapping multi-component systems, while the second numerical experiment explored when the two models are equivalent. These experiments were conducted at loading factor LF of 2% and 1%, respectively, as defined by Chen, et al. [3], which were used to calculate the injection time t_{inj}:

$$\mathrm{LF} = \frac{\nu + \sigma}{\Lambda} \cdot c_{\mathrm{inj}} \cdot u \cdot t_{\mathrm{inj}} \Big/ L \tag{12}$$

In the third numerical experiment, we evaluated the effect of LF changes within the range of 0.5%, 1%, 2%, 4%, 8%, and 16% on chromatograms.

Table 4 presents the model parameters used in numerical experiments. The operating parameters for single-component and overlapping multi-component systems were referenced from Chen, et al. [4] and Chen, et al. [3], respectively. The parameters for non-overlapping multi-component systems were obtained by modifying the linear parameter k_{eq}. Considering the reported values of interaction parameters in the literature [5-9], $k_{\mathrm{s}} = -5\ \mathrm{M}^{-1}$ and $k_{\mathrm{p}} = 15,000\ \mathrm{M}^{-1}$ were chosen to ensure that both interaction parameters affect activity, rather than one dominating over the other. Their ratio was obtained by setting Eq. (3) to approach zero:

$$-\frac{k_{\mathrm{p}}}{k_{\mathrm{s}}} = \frac{c_{\mathrm{s}}}{c_{\mathrm{p}}} = \frac{0.5 \times \left(c_{\mathrm{final}} + c_{\mathrm{initial}}\right)}{c_{\mathrm{inj}}} = \frac{0.5 \times (0.55 + 0.05)}{0.0001} = 3000 \tag{13}$$

where c_{initial} and c_{final} are the salt concentrations at the initial and final gradients, respectively. The selected values and ratio of the interaction parameters are considered reasonable as they lie around the logarithmic midpoint of the reported values [5-9], thus comprehensively reflecting the variability of interaction parameters across different systems.

3.2. Column models

The column model in numerical experiments employed the equilibrium dispersive model as:

$$\frac{\partial c_i}{\partial t}(z,t) = -\frac{u}{\varepsilon_{\mathrm{t}}}\frac{\partial c_i}{\partial z}(z,t) + D_{\mathrm{app}}\frac{\partial^2 c_i}{\partial z^2}(z,t) - \frac{1-\varepsilon_{\mathrm{t}}}{\varepsilon_{\mathrm{t}}}\frac{\partial q_i}{\partial t}(z,t) \tag{14}$$

where z and t are axial position and time, respectively. Eq. (14) was completed with Danckwerts and Neumann boundary conditions at the column inlet and outlet, respectively:

$$-\frac{\varepsilon_{\mathrm{t}} D_{\mathrm{app}}}{u_{\mathrm{col}}}\frac{\partial c_i}{\partial z}(0,t) + c_i(0,t) = \begin{cases} c_{\mathrm{inj},i} & 0 < t \le t_{\mathrm{inj}} \\ 0 & t > t_{\mathrm{inj}} \end{cases} \tag{15}$$

$$\frac{\partial c_i}{\partial z}(L,t) = 0 \tag{16}$$

The unnamed symbols can be referred in Table 4.

4. Results

Fig. 1A illustrates the simulated chromatograms of our proposed model and the reference model in overlapping multi-component systems. In both model simulations, the elution behavior of impurity W appears similar, while the product P and impurity S exhibit significant differences. Particularly with impurity S, a peak shoulder simulated by our model can be observed, whereas the peak shape of the reference model is nearly symmetric. Additionally, in Fig. 1A, the peak height simulated by our model decreases with increasing retention time, in contrast to the reference model.

Compared to the reference model, the activity at retention time in our model approaches one. This is because our model considers contributions to activity from all solute molecules (all components and modifiers), rather than just one specific components.

Table 4

Model parameters of numerical experiments for single-component, overlapping multi-component, and non-overlapping multi-component systems.

Parameters	Unit	Symbol	Single solute	Overlapping multi solutes	Non-overlapping multi solutes
Column length	cm	L	25.0		
Total porosity	–	ε_{t}	0.58		
Capacity	M	Λ	0.57		
Injection concentration	M	c_{inj}	1E-4	[1E-4, 1E-4, 1E-4]	[1E-4, 1E-4, 1E-4]
Initial salt concentration	M	c_{initial}	0.05		
Final salt concentration	M	c_{final}	0.55		
Apparent axial dispersion	mm^2/s	D_{app}	0.21		
Velocity	mm/s	u	0.278		
Graident length	CV	–	8.0		
Characteristic charge	–	ν	7.00	[6.00, 7.00, 8.00]	[6.00, 7.00, 8.00]
Equilibrium coefficient	–	k_{eq}	0.200	[0.100, 0.200, 0.400]	[0.020, 0.200, 2.0]
Shielding factor	–	σ	50.5	[51.0, 50.0, 49.0]	[51.0, 50.0, 49.0]
Kinetic coefficient	sM^{ν}	k_{kin}	0.100	[0.100, 0.100, 0.100]	[0.100, 0.100, 0.100]
Priotein-salt interaction	M^{-1}	k_{s}	−5	[−5, −5, −5]	[−5, −5, −5]
Priotein-protein interaction	M^{-1}	k_{p}	15,000	[−15,000, −15,000, −15,000]	[−15,000, −15,000, −15,000]

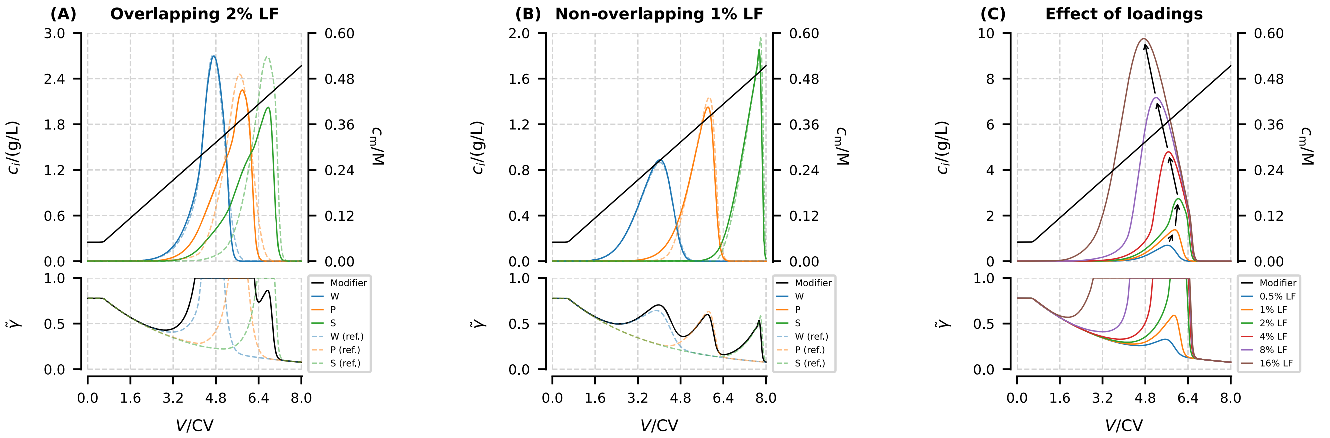

Fig. 1. Simulated chromatograms (top) and activity curves (bottom) of the multi-component Mollerup model (solid lines) and the reference model (dashed lines) in overlapping (A) and non-overlapping (B) multi-component systems. Effect of loadings on simulated chromatograms in single-component systems (C).

As the overlapping area decreases, both models exhibit similar chromatograms, as shown in Fig. 1B. This implies that when there is no overlap, the chromatograms simulated by these models are equivalent, which is evidently determined by their expressions (our model in Eq. (6) and the reference model in Eq. (4)). However, in practical applications of multi-component systems, situations without overlap are practically unattainable. Hence, our model and the reference model are entirely distinct in such applications.

In the single-component systems, our model and the reference model are equivalent to the single-component Mollerup model, because their chromatograms completely align (Fig. 1C). This result also reveals that with increasing loading, the retention time exhibits a trend of initial increase followed by decrease, termed as anti-Langmuirian to Langmuirian elution behavior.

5. Discussion

Considering the results of numerical experiments, we can assert that our proposed model exhibits significant differences from the reference model in multi-component chromatographic modeling. Our model considers the contributions of all solute molecules (all components and modifiers) to activity, elucidating the intermolecular interactions inherent in the activity definition. This model aligns more closely with thermodynamic consistency and coherence with the van der Waals equation of state. This indicates that our model represents a thermodynamically consistent generalization of the single-component Mollerup model to multi-component systems. Conversely, the reference model, which solely considers the contribution of individual component to activity, deviates from the principles of thermodynamic consistency.

However, the investigation in this study employs a simplified version of the multi-component Mollerup model ($\bar{k}_s c_s + \bar{k}_p \sum_{j=1}^{n} c_j$), assuming complete uniformity of two interaction parameters (k_s and k_p) for all components. While this assumption ease the complexity of the investigation, they also limit the exploration of the full potential of the multi-component Mollerup model. This exploration will be further performed in the future research.

Mechanistic modeling indicates that the models should align with underlying mechanisms. Hence, we advocate adopting of the multi-component Mollerup model for activity modeling in multi-component chromatographic separation to enhance thermodynamic consistency. Unfortunately, a significant challenge arises as the multi-component Mollerup model cannot be simplified into the reference model, which means that users of the reference model (with over 40 direct applications and 442 citations) transitioning to the multi-component Mollerup model must contend with a change in the number of parameters. To facilitate a smooth transition, one solution is to utilize alternative models (Table 3) simplified from the multi-component Mollerup model.

6. Conclusion

In this work, the asymmetric activity model for multi-component systems was rederived and termed the multi-component Mollerup model, using the van der Waals equation of state. In contrast to the reference model, our proposed model accounts for the contributions of all solute molecules (all components and modifiers) to the activity. The results of three numerical experiments indicate that our proposed model represents a thermodynamically consistent generalization of the single-component Mollerup model to multi-component systems.

CRediT authorship contribution statement

Yu-Cheng Chen: Writing – original draft, Visualization, Validation, Software, Methodology, Investigation, Funding acquisition, Formal analysis, Data curation, Conceptualization. **Shan-Jing Yao:** Writing – review & editing, Supervision, Resources. **Dong-Qiang Lin:** Writing – review & editing, Supervision, Resources, Project administration, Funding acquisition.

Declaration of competing interest

The authors declare that they have no known competing financial interests or personal relationships that could have appeared to influence the work reported in this paper.

Data availability

Data will be made available on request.

Acknowledgments

This work was supported by the National Natural Science Foundation of China (22078286), Zhejiang Key Science and Technology Project (2023C03116), Huadong Medicine Joint Funds of the Zhejiang Provincial Natural Science Foundation of China (LHDMZ24B060001), and China Scholarship Council (CSC, no. 202306320355).

Supplementary materials

Supplementary material associated with this article can be found, in the online version, at doi:10.1016/j.chroma.2024.465156.

References

[1] J.M. Mollerup, Applied thermodynamics: a new frontier for biotechnology, Fluid. Phase Equilib. 241 (2006) 205–215, https://doi.org/10.1016/j.fluid.2005.12.037.

[2] J.M. Prausnitz, R.N. Lichtenthaler, E.G. De Azevedo, Molecular Thermodynamics of Fluid-Phase Equilibria, Pearson Education, 1998.

[3] Y.-C. Chen, S.-J. Yao, D.-Q. Lin, Parameter-by-parameter method for steric mass action model of ion exchange chromatography: simplified estimation for steric shielding factor, J. Chromatogr. A 1687 (2023) 463655, https://doi.org/10.1016/j.chroma.2022.463655.

[4] Y.-C. Chen, S.-J. Yao, D.-Q. Lin, Parameter-by-parameter method for steric mass action model of ion exchange chromatography: theoretical considerations and experimental verification, J. Chromatogr. A 1680 (2022) 463418, https://doi.org/10.1016/j.chroma.2022.463418.

[5] B.K. Nfor, M. Noverraz, S. Chilamkurthi, P. Verhaert, L.A.M. van der Wielen, M. Ottens, High-throughput isotherm determination and thermodynamic modeling of protein adsorption on mixed mode adsorbents, J. Chromatogr. A 1217 (2010) 6829–6850, https://doi.org/10.1016/j.chroma.2010.07.069.

[6] B.K. Nfor, D.S. Zuluaga, P.J.T. Verheijen, P. Verhaert, L.A.M. van der Wielen, M. Ottens, Model-based rational strategy for chromatographic resin selection, Biotechnol. Prog. 27 (2011) 1629–1643, https://doi.org/10.1002/btpr.691.

[7] J. Wang, E.W. Jenkins, J.R. Robinson, A. Wilson, S.M. Husson, A new multimodal membrane adsorber for monoclonal antibody purifications, J. Memb. Sci 492 (2015) 137–146, https://doi.org/10.1016/j.memsci.2015.05.013.

[8] M. Moreno-González, P. Chuekitkumchorn, M. Silva, R. Groenewoud, High throughput process development for the purification of rapeseed proteins napin and cruciferin by ion exchange chromatography, Food Bioprod. Process. 125 (2021) 228–241, https://doi.org/10.1016/j.fbp.2020.11.011.

[9] J. Koch, D. Scheps, M. Gunne, O. Boscheinen, M. Hafner, C. Frech, Mechanistic modeling and simulation of a complex low and high loading elution behavior of a polypeptide in cation exchange chromatography, J. Sep. Sci. 45 (2022) 2008–2023, https://doi.org/10.1002/jssc.202200098.

[10] K. Westerberg, N. Borg, N. Andersson, B. Nilsson, Supporting design and control of a reversed-phase chromatography step by mechanistic modeling, Chem. Eng. Technol. 35 (2012) 169–175, https://doi.org/10.1002/ceat.201000505.

[11] K. Arkell, M.P. Breil, S.S. Frederiksen, B. Nilsson, Mechanistic modeling of reversed-phase chromatography of insulins with potassium chloride and ethanol as mobile-phase modulators, ACS. Omega 2 (2017) 136–146, https://doi.org/10.1021/acsomega.6b00248.

[12] K. Arkell, M.P. Breil, S.S. Frederiksen, B. Nilsson, Mechanistic modeling of reversed-phase chromatography of insulins within the temperature range 10-40 °C, ACS. Omega 3 (2018) 1946–1954, https://doi.org/10.1021/acsomega.7b01527.

[13] K. Arkell, H.K. Knutson, S.S. Frederiksen, M.P. Breil, B. Nilsson, Pareto-optimal reversed-phase chromatography separation of three insulin variants with a solubility constraint, J. Chromatogr. A 1532 (2018) 98–104, https://doi.org/10.1016/j.chroma.2017.11.065.

[14] J.M. Mollerup, The thermodynamic principles of ligand binding in chromatography and biology, J. Biotechnol. 132 (2007) 187–195, https://doi.org/10.1016/j.jbiotec.2007.05.036.

[15] J.M. Mollerup, A review of the thermodynamics of protein association to ligands, protein adsorption, and adsorption isotherms, Chem. Eng. Technol. 31 (2008) 864–874, https://doi.org/10.1002/ceat.200800082.

[16] R.W. Deitcher, J.E. Rome, P.A. Gildea, J.P. O'Connell, E.J. Fernandez, A new thermodynamic model describes the effects of ligand density and type, salt concentration and protein species in hydrophobic interaction chromatography, J. Chromatogr. A 1217 (2010) 199–208, https://doi.org/10.1016/j.chroma.2009.07.068.

[17] K. Westerberg, E.B. Hansen, M. Degerman, T.B. Hansen, B. Nilsson, Model-based process challenge of an industrial ion-exchange chromatography step, Chem. Eng. Technol. 35 (2012) 183–190, https://doi.org/10.1002/ceat.201000560.

[18] B.K. Nfor, T. Ahamed, M.W.H. Pinkse, L.A.M. van der Wielen, P. Verhaert, G.W. K. van Dedem, M.H.M. Eppink, E. van de Sandt, M. Ottens, Multi-dimensional fractionation and characterization of crude protein mixtures: toward establishment of a database of protein purification process development parameters, Biotechnol. Bioeng. 109 (2012) 3070–3083, https://doi.org/10.1002/bit.24576.

[19] B.K. Nfor, J. Ripic, A. van der Padt, M. Jacobs, M. Ottens, Model-based high-throughput process development for chromatographic whey proteins separation, Biotechnol. J. 7 (2012) 1221–1232, https://doi.org/10.1002/biot.201200191.

[20] B.K. Nfor, T. Ahamed, G.W.K. van Dedem, P. Verhaert, L.A.M. van der Wielen, M. H.M. Eppink, E. van de Sandt, M. Ottens, Model-based rational methodology for protein purification process synthesis, Chem. Eng. Sci. 89 (2013) 185–195, https://doi.org/10.1016/j.ces.2012.11.034.

[21] S. Chilamkurthi, D.M. Sevillano, L.H.G. Albers, M.R. Sahoo, P.J.T. Verheijen, L.A. M. van der Wielen, J.L. den Hollander, M. Ottens, Thermodynamic description of peptide adsorption on mixed-mode resins, J. Chromatogr. A 1341 (2014) 41–49, https://doi.org/10.1016/j.chroma.2014.03.031.

[22] A. Holmqvist, C. Andersson, F. Magnusson, J. Åkesson, Methods and tools for robust optimal control of batch chromatographic separation processes, Processes 3 (2015) 568–606, https://doi.org/10.3390/pr3030568.

[23] M.R. Mirani, F. Rahimpour, Thermodynamic modelling of hydrophobic interaction chromatography of biomolecules in the presence of salt, J. Chromatogr. A 1422 (2015) 170–177, https://doi.org/10.1016/j.chroma.2015.10.019.

[24] A.B. Wilson, E.W. Jenkins, J. Wang, Numerical simulation of chemical separations using multimodal adsorption isotherms, Results Appl. Math. 7 (2020) 100122, https://doi.org/10.1016/j.rinam.2020.100122.

[25] A.T. Hanke, E. Tsintavi, M.D.R. Vazquez, L.A.M. van der Wielen, P. Verhaert, M.H. M. Eppink, E. van de Sandt, M. Ottens, 3D-liquid chromatography as a complex mixture characterization tool for knowledge-based downstream process development, Biotechnol. Prog. 32 (2016) 1283–1291, https://doi.org/10.1002/btpr.2320.

[26] A. Holmqvist, F. Magnusson, Open-loop optimal control of batch chromatographic separation processes using direct collocation, J. Process. Control 46 (2016) 55–74, https://doi.org/10.1016/j.jprocont.2016.08.002.

[27] Y.F. Lee, H. Graalfs, C. Frech, Thermodynamic modeling of protein retention in mixed-mode chromatography: an extended model for isocratic and dual gradient elution chromatography, J. Chromatogr. A 1464 (2016) 87–101, https://doi.org/10.1016/j.chroma.2016.08.026.

[28] T.C. Huuk, T. Hahn, K. Doninger, J. Griesbach, S. Hepbildikler, J. Hubbuch, Modeling of complex antibody elution behavior under high protein load densities in ion exchange chromatography using an asymmetric activity coefficient, Biotechnol. J. 12 (2017) 1600336, https://doi.org/10.1002/biot.201600336.

[29] Y.F. Lee, S. Kluters, M. Hillmann, T. von Hirschheydt, C. Frech, Modeling of bispecific antibody elution in mixed-mode cation-exchange chromatography, J. Sep. Sci. 40 (2017) 3632–3645, https://doi.org/10.1002/jssc.201700313.

[30] S.M. Pirrung, L.A.M. van der Wielen, R.F.W.C. van Beckhoven, E.J.A.X. van de Sandt, M.H.M. Eppink, M. Ottens, Optimization of biopharmaceutical downstream processes supported by mechanistic models and artificial neural networks, Biotechnol. Prog. 33 (2017) 696–707, https://doi.org/10.1002/btpr.2435.

[31] S.M. Pirrung, D.P. da Cruz, A.T. Hanke, C. Berends, R. van Beckhoven, M.H. M. Eppink, M. Ottens, Chromatographic parameter determination for complex biological feedstocks, Biotechnol. Prog. 34 (2018) 1006–1018, https://doi.org/10.1002/btpr.2642.

[32] T. Briskot, F. Stuckler, F. Wittkopp, C. Williams, J. Yang, S. Konrad, K. Doninger, J. Griesbach, M. Bennecke, S. Hepbildikler, J. Hubbuch, Prediction uncertainty assessment of chromatography models using Bayesian inference, J. Chromatogr. A 1587 (2019) 101–110, https://doi.org/10.1016/j.chroma.2018.11.076.

[33] S. Andris, J. Hubbuch, Modeling of hydrophobic interaction chromatography for the separation of antibody-drug conjugates and its application towards quality by design, J. Biotechnol. 317 (2020) 48–58, https://doi.org/10.1016/j.jbiotec.2020.04.018.

[34] H.G. Bock, D.H. Cebulla, C. Kirches, A. Potschka, Mixed-integer optimal control for multimodal chromatography, Comput. Chem. Eng. 153 (2021) 107435, https://doi.org/10.1016/j.compchemeng.2021.107435.

[35] E. Lietta, A. Pieri, A.G. Cardillo, M. Vanni, R. Pisano, A.A. Barresi, An experimental and modeling combined approach in preparative hydrophobic interaction chromatography, Processes 10 (2022) 1027, https://doi.org/10.3390/pr10051027.

[36] F. Seelinger, F. Wittkopp, T. von Hirschheydt, C. Frech, Anti-Langmuir elution behavior of a bispecific monoclonal antibody in cation exchange chromatography: mechanistic modeling using a pH-dependent Self-Association Steric Mass Action isotherm, J. Chromatogr. A 1689 (2023) 463730, https://doi.org/10.1016/j.chroma.2022.463730.

[37] M. Mouellef, F.L. Vetter, J. Strube, Benefits and limitations of artificial neural networks in process chromatography design and operation, Processes 11 (2023) 1115, https://doi.org/10.3390/pr11041115.

[38] J. Koch, D. Scheps, M. Gunne, O. Boscheinen, C. Frech, Mechanistic modeling of cation exchange chromatography scale-up considering packing inhomogeneities, J. Sep. Sci. 46 (2023) 2300031, https://doi.org/10.1002/jssc.202300031.

[39] R. Hess, D. Yun, D. Saleh, T. Briskot, J.-H. Grosch, G. Wang, T. Schwab, J. Hubbuch, Standardized method for mechanistic modeling of multimodal anion exchange chromatography in flow through operation, J. Chromatogr. A 1690 (2023) 463789, https://doi.org/10.1016/j.chroma.2023.463789.

[40] T. Hahn, T. Trunzer, F. Rusly, R. Zolyomi, L.K. Shekhawat, G. Malmquist, A. Hesslein, H. Tjandra, Predictive scaling of fiber-based protein A capture chromatography using mechanistic modeling, Biotechnol. Bioeng. (2023), https://doi.org/10.1002/bit.28434.

[41] T. Hahn, N. Geng, K. Petrushevska-Seebach, M.E. Dolan, M. Scheindel, P. Graf, K. Takenaka, K. Izumida, L. Li, Z. Ma, N. Schuelke, Mechanistic modeling, simulation, and optimization of mixed-mode chromatography for an antibody polishing step, Biotechnol. Prog. 39 (2023) e3316, https://doi.org/10.1002/btpr.3316.

[42] S.H. Altern, J.P. Welsh, J.Y. Lyall, A.J. Kocot, S. Burgess, V. Kumar, C. Williams, A. M. Lenhoff, S.M. Cramer, Isotherm model discrimination for multimodal chromatography using mechanistic models derived from high-throughput batch isotherm data, J. Chromatogr. A 1693 (2023) 463878, https://doi.org/10.1016/j.chroma.2023.463878.

[43] R. Hess, J. Faessler, D. Yun, A. Mama, D. Saleh, J.-H. Grosch, G. Wang, T. Schwab, J. Hubbuch, Predicting multimodal chromatography of therapeutic antibodies using multiscale modeling, J. Chromatogr. A 1718 (2024) 464706, https://doi.org/10.1016/j.chroma.2024.464706.

[44] Y.-X. Yang, Y.-C. Chen, S.-J. Yao, D.-Q. Lin, Parameter-by-parameter estimation method for adsorption isotherm in hydrophobic interaction chromatography, J. Chromatogr. A 1716 (2024) 464638, https://doi.org/10.1016/j.chroma.2024.464638.

[45] S.H. Altern, J.Y. Lyall, J.P. Welsh, S. Burgess, V. Kumar, C. Williams, A.M. Lenhoff, S.M. Cramer, High-throughput in silico workflow for optimization and characterization of multimodal chromatographic processes, Biotechnol. Prog. (2024) e3483, https://doi.org/10.1002/btpr.3483.

[46] Y.-X. Yang, Z.-Y. Lin, Y.-C. Chen, S.-J. Yao, D.-Q. Lin, Modeling multi-component separation in hydrophobic interaction chromatography with improved parameter-by-parameter estimation method, J. Chromatogr. A 1730 (2024) 465121, https://doi.org/10.1016/j.chroma.2024.465121.